

## Time-resolved photoluminescence investigations of electric-field domain formation in GaAs-AlAs superlattices

R. Klann, S. H. Kwok, H. T. Grahn, and R. Hey

*Paul-Drude-Institut für Festkörperelektronik, Hausvogteiplatz 5-7, D-10117 Berlin, Germany*

(Received 17 May 1995)

The electric-field domain-formation time of an undoped GaAs-AlAs superlattice embedded in a  $p^+i-n^+$  diode is investigated by time-resolved photoluminescence (PL). After optical excitation of electron-hole pairs with an ultrashort light pulse, the previously homogeneous electric field breaks up into domains that can be observed by a splitting of the PL line due to the quantum-confined Stark effect. The PL dynamics is studied as a function of excitation density and applied voltage. A domain-formation time on the order of a few nanoseconds is found. This time is unexpectedly short compared to the vertical transport time of electrons through the entire superlattice.

The electric field across a weakly coupled superlattice is homogeneous if the carrier density within the quantum wells is low. Under strong photoexcitation, the superlattice breaks up into two domains with different field strengths.<sup>1</sup> Domains are separated by a space-charge layer with a density governed by Poisson's equation. They are ordered in such a way that the high-field domain is located near the anode.<sup>1,2</sup> The formation of electric-field domains is related to an instability due to negative differential resistance (NDR) arising from resonant tunneling.<sup>1,3-11</sup> The basic features of domain formation have been recently described by theoretical models.<sup>1,12-15</sup> In cw photoluminescence (PL) experiments, the two distinct field strengths are visible through their different Stark shifts leading to two clearly separated PL lines.<sup>1</sup> Therefore, the field strengths and the spatial extent of the domains can be determined directly from the energies and intensities of the PL peaks, respectively.

In this work, we investigate the evolution of the field distribution in an undoped superlattice by time-resolved PL after intense pulsed excitation. We find that for high-power photoexcitation two stable domains are formed within several nanoseconds. This is unexpectedly short compared with the typical transit time of about one hundred nanoseconds across a weakly coupled superlattice<sup>16</sup> and previous switch-on experiments of domain formation.<sup>17</sup> These observations can be explained by a model incorporating negative differential resistance and charge fluctuations within the superlattice.

The investigated GaAs-AlAs superlattice is grown by molecular-beam epitaxy on a  $n^+$ -type GaAs(001) substrate. The 50 periods of a 14.4-nm GaAs well and a 3.4-nm AlAs barrier represent the  $\sim 1\text{-}\mu\text{m}$ -thick intrinsic region of a  $p^+i-n^+$  diode. The contact layers consist of heavily carbon- and silicon-doped  $\text{Al}_{0.5}\text{Ga}_{0.5}\text{As}$  layers and are transparent at the emitting wavelengths. Cylindrical diode structures with a diameter of 230  $\mu\text{m}$  are processed out of the wafer by mesa etching techniques. The  $p^+$  region on top is supplied with an Ohmic contact using Au/Be, while the substrate is contacted with AuGe/Ni ( $n^+$  region). A Keithley 236 source measure unit is used for  $I$ - $V$  characterization. For stationary PL and photocurrent measurements we excite with a cw Ti:sapphire laser at a wavelength of 720 nm. Time-resolved PL measure-

ments are performed using a streak-camera system in single-shot operation in conjunction with a pulsed femtosecond Ti:sapphire laser (Coherent Mira) tuned to 740 nm. The repetition rate is reduced to 500 kHz by a pulse picker to avoid carrier accumulation effects. We carefully checked that no carriers are present in the superlattice before the excitation, i.e., that the initial electric field is homogeneous. This was achieved by reducing the repetition rate of the excitation until only one single narrow PL peak was present before the excitation pulse arrived. To overcome carrier recombination, which quenches the PL signal within several tens of nanoseconds, we applied an additional weak cw background excitation with a HeNe laser. The excitation density is adjusted by neutral density filters and monitored by the photocurrent. The typical size of the laser spot is  $\sim 100\ \mu\text{m}$ . The luminescence is dispersed by a 22-cm monochromator (1200 lines/mm grating) and focused onto the photocathode of the streak tube. The streak images are recorded by a cooled charge-coupled device array and are further processed by a computer. The spectral resolution amounts to 0.4 nm, and the temporal resolution of the single-shot system is 50 ps. The samples are mounted on the cold finger of a He flow cryostat. All measurements are performed at 5 K.

For weak excitation the  $I$ - $V$  characteristic exhibits a pronounced NDR region due to tunneling resonance between the first and the second subband in adjacent wells [see Fig. 1(a)].<sup>18,19</sup> The shoulders at  $-0.5$  and  $-1.5$  V are related to phonon-assisted tunneling.<sup>20</sup> For large excitation densities the corresponding  $I$ - $V$  curve is shown in Fig. 1(b). The diagram can be divided into three regions, namely, I-II, II-III, and transition region TR. Domains I and II coexist in the I-II region, while domains II and III coexist in the II-III region. Domains I, II, and III are associated with the  $C_1 \rightarrow C_1$ ,  $C_1 \rightarrow C_2$ , and  $C_1 \rightarrow C_3$  tunneling resonances, respectively, where  $C_i$  denotes the  $i$ th conduction subband. The field strength of the high-field domain in region TR was shown to be below the tunneling resonance condition.<sup>21</sup> The sawtooth-like  $I$ - $V$  characteristic demonstrates the existence of two domains. The current jumps are related to the movement of the domain boundary through the superlattice as the voltage increases.

In the I-II region, the PL peaks associated with the domains I and II cannot be spectrally resolved. However, two

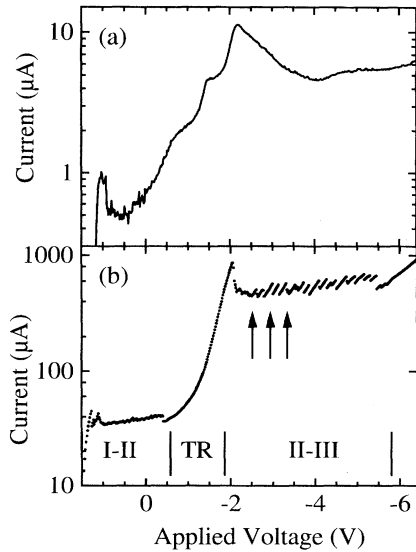


FIG. 1. The  $I$ - $V$  characteristics of the superlattice under cw excitation at 5 K [power: (a) 0.05 mW, (b) 25 mW]. The arrows in (b) mark the voltages for the PL spectra in Fig. 2. The symbols I-II, TR, and II-III are described in the text.

well-separated PL peaks are seen in the II-III region. In Fig. 2, PL spectra of the  $C_1H_1$  emission are shown for three reverse bias voltages in the II-III region.  $H_j$  denotes the  $j$ th hole subband. The spectra were recorded 5 ns after excitation with a photon energy of 1.675 eV (average excitation power 1 mW). The three PL spectra were measured at the voltages marked by arrows in Fig. 1(b). The emission associated with the high-field domain is redshifted by the quantum-confined Stark effect.<sup>22,23</sup> With increasing electric field, i.e., from  $-2.5$  to  $-3.3$  V, the high-field domain expands. This expan-

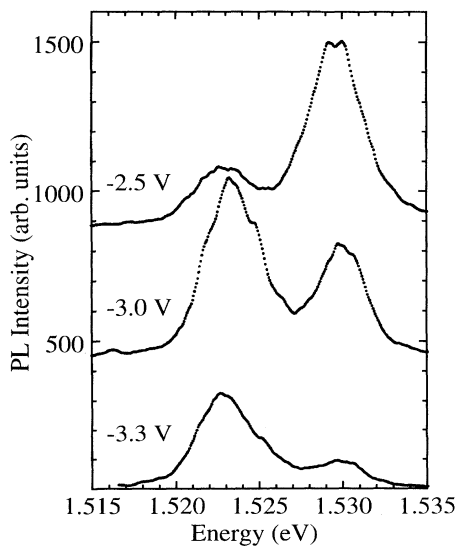


FIG. 2. PL spectra 5 ns after excitation at 5 K for three different applied voltages [marked in Fig. 1(b), average excitation power 1 mW]. The spectra have been shifted vertically for better visibility.

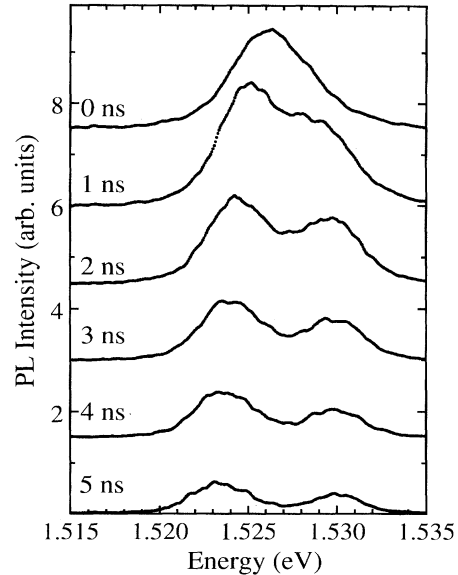


FIG. 3. Time-resolved PL spectra at 5 K for different delay times. The spectra have been shifted vertically (applied voltage  $-3.0$  V, average excitation power 1 mW).

sion results in a higher intensity of the PL peak at lower energy (1.523 eV). This behavior has already been observed in cw PL experiments.<sup>1</sup> However, there is a very pronounced difference between cw and pulsed excitation concerning the width of the voltage range, in which two domain peaks are found. In cw experiments we find the splitting of the  $C_1H_1$  emission into two domain peaks in the entire voltage range where the sawtoothlike  $I$ - $V$  characteristic persists [from  $-2.0$  to  $-6.0$  V, see Fig. 1(b)]. In time-resolved experiments, however, the splitting of the PL emission is limited to the range  $-2.0$  to  $-3.7$  V. This voltage region coincides with the NDR range [see Fig. 1(a)]. From  $-3.7$  to  $-6.0$  V only one broad peak is seen for the first 20 ns after excitation. As mentioned earlier we are able to detect the PL signal only for several tens of nanoseconds, because of carrier transport and relaxation processes. However, due to the fact that in cw experiments a line splitting is observed, we conclude that in this positive differential resistance region the domain formation time is much longer than 20 ns.

We will now discuss the time evolution of the PL spectra after pulsed excitation. Typical spectra at various delay times for an applied voltage of  $-3.0$  V are shown in Fig. 3. The spectra are integrated over 150 ps. At  $t = 0$  ns only a single broad PL line is present. The energetic position of this maximum corresponds to the expected  $C_1H_1$  transition energy in a homogeneous electric field. The single line evolves into two peaks within two nanoseconds. The PL intensities of the peaks decrease because of carrier recombination and transport. The peak at 1.530 eV (low-field domain) stays at the same energetic position at later times, while the high-field peak shifts 2 meV to the red with increasing time delay. The formation time does not exhibit a strong dependence on the applied voltage between  $-2.0$  and  $-3.7$  V.

The separation of both peaks not only on the delay time, but also on the excitation power, i.e., the initial

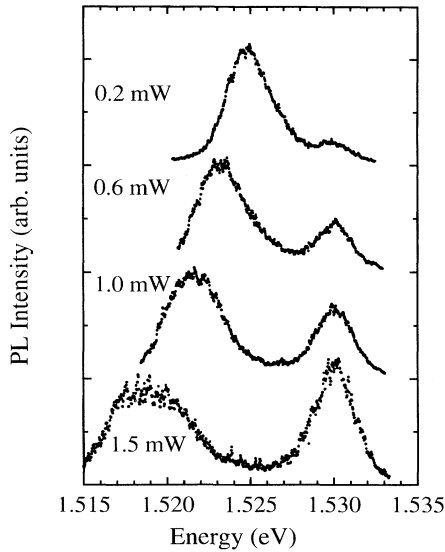


FIG. 4. PL spectra at  $-3.2$  V for different excitation powers 10 ns after excitation at 5 K. The spectra have been shifted vertically.

carrier density. Four PL spectra recorded 10 ns after excitation are shown in Fig. 4 for averaged excitation powers between 0.2 and 1.5 mW. With increasing excitation density the separation between the low- and high-field domain peaks increases. Again we find that only the high-field domain peak shifts toward lower energies with increasing excitation. The low-field domain peak remains at the same energy. The intensity ratio of the two peaks also changes with excitation power. For low intensities, the high-field domain peak dominates. With increasing power the low-field domain peak gains in intensity, and for 1.5 mW it is even stronger than the high-field domain peak. The experimental data suggest that for a fixed applied voltage with increasing excitation intensity the domain boundary shifts vertically in depth towards the substrate side. With increasing carrier density, the domain boundary is charged up and shifted towards the anode increasing the field strength and decreasing the spatial extent of the high-field domain. The two-dimensional charge density at the boundary ( $\sigma$ ) is estimated from the field strengths of the two domains, which are derived from the Stark shift of the PL lines (see Fig. 4).  $\sigma$  is calculated by substituting these field strengths in Poisson's equation. A linear dependence between  $\sigma$  and the excitation power density is found.

Our observations can be understood by a qualitative argument. In the NDR region, the drift velocity of an electron decreases as the field increases. As a result, a local small charge fluctuation will lead to the buildup of a space-charge layer, the domain boundary, until two stable domains are formed. The relationship between  $\sigma$  and the domain formation time ( $t_f$ ) can be expressed as

$$\begin{aligned} \sigma &= \int_0^{t_f} e \{ n_{\text{LF}}(t) v [F_{\text{LF}}(t)] - n_{\text{HF}}(t) v [F_{\text{HF}}(t)] \} dt \\ &= \int_0^{t_f} \Delta J(t) dt, \end{aligned} \quad (1)$$

where  $n_{\text{LF}}$  ( $n_{\text{HF}}$ ) is the three-dimensional electron density and  $v(F_{\text{LF}})$  [ $v(F_{\text{HF}})$ ] is the drift velocity of electrons within

the low-field (high-field) domain.  $\Delta J$  is the difference between the current densities of the two domains.  $n_{\text{LF}}$  and  $n_{\text{HF}}$  depend mainly on the carrier lifetime. Stable domains are formed when  $\Delta J(t_f) = 0$ . The domain formation time can be estimated by taking  $\sigma \approx 2 \times 10^{11} \text{ cm}^{-2}$  and the measured transient current density as  $2.5 \text{ A cm}^{-2}$ . The typical domain formation time is estimated to be less than 12 ns, which is consistent with our observation. From Eq. (1), it is also clear that  $\sigma$  is proportional to the carrier concentration within the wells.

The spatial shift of the domain boundary as a function of power density can be attributed to absorption saturation effects. The initial excitation density in our experiments is estimated to be larger than  $10^{12} \text{ cm}^{-2}$  even for 0.2 mW. At low excitation power and under reverse bias, the carrier density decreases exponentially from the cathode at the top contact to the anode. The second derivative of the carrier density vs the depth is positive. Small charge fluctuations will build up field inhomogeneities preferentially in the region of the largest derivative of the carrier density [see Eq. (1)], which is near the cathode. Therefore, the domain boundary is formed near the cathode and the spatial extent of the high-field domain is large. At high powers, however, the carrier density is rather uniform throughout the first part of the superlattice due to a saturation of the absorption. Near the anode the excitation density is reduced below the saturation value due to the strong absorption within the first part of the superlattice. Now the carrier density decreases faster near the anode, i.e., the second derivative of the carrier density vs depth is changing its sign. This favors a buildup of the domain boundary near the anode. Consequently, the spatial extent of the high-field domain is now smaller and the electric field is higher than for lower excitation densities. Model calculations accounting for saturation effects are in agreement with our experimental data.

The main differences between the previous work (Ref. 17) and the current investigation is the excitation condition. While in Ref. 17 a steplike excitation was used, in this work the carriers are excited by an ultrafast light pulse. Therefore, the excitation power differs by about two orders of magnitude between these two excitation conditions. Furthermore, the system responds for a steplike excitation in a way similar to that for cw excitation. However, the excitation by a light pulse is very different from the cw case.

In conclusion, we have studied the formation time of electric-field domains in an undoped superlattice by time-resolved PL technique. Using pulsed excitation, an initial carrier concentration above  $10^{12} \text{ cm}^{-2}$  within the quantum wells is created. We demonstrate that the uniform field distribution of superlattices can be transformed into two well-defined domains within several nanoseconds as long as the applied voltage corresponds to the negative differential resistance region. In the positive differential resistance region, however, the domain formation time exceeds 20 ns. The results are explained by a model describing the charging of the domain boundary.

We would like to thank M. H6ricke for expert technical assistance in sample growth, E. Wiebcke for processing the diodes, and J. Kastrup and A. Wacker for valuable discussions.

- <sup>1</sup>H.T. Grahn, H. Schneider, and K. v. Klitzing, *Appl. Phys. Lett.* **54**, 1757 (1989); *Phys. Rev. B* **41**, 2890 (1990).
- <sup>2</sup>S.H. Kwok, U. Jahn, J. Menniger, H.T. Grahn, and K. Ploog, *Appl. Phys. Lett.* **66**, 2113 (1995).
- <sup>3</sup>L. Esaki and L.L. Chang, *Phys. Rev. Lett.* **33**, 495 (1974).
- <sup>4</sup>Y. Kawamura, K. Wakita, H. Asaki, and K. Kurumada, *Jpn. J. Appl. Phys.* **25**, L928 (1986).
- <sup>5</sup>K.K. Choi, B.F. Levine, R.J. Malik, J. Walker, and C.G. Bethea, *Phys. Rev. B* **35**, 4172 (1987).
- <sup>6</sup>M. Helm, P. England, E. Colas, F. DeRosa, and S.J. Allen, Jr., *Phys. Rev. Lett.* **63**, 74 (1989).
- <sup>7</sup>T.H.H. Vuong, D.C. Tsui, and W.T. Tsang, *J. Appl. Phys.* **66**, 3688 (1989).
- <sup>8</sup>H.T. Grahn, R.J. Haug, W. Müller, and K. Ploog, *Phys. Rev. Lett.* **67**, 1618 (1991).
- <sup>9</sup>Y. Zhang, Y. Li, D. Jiang, X. Yang, and P. Zhang, *Appl. Phys. Lett.* **64**, 3416 (1994).
- <sup>10</sup>J. Kastrop, H.T. Grahn, K. Ploog, F. Prengel, A. Wacker, and E. Schöll, *Appl. Phys. Lett.* **65**, 1808 (1994).
- <sup>11</sup>Z.Y. Han, S.F. Yoon, K. Radhakrishnan, and D.H. Zhang, *Appl. Phys. Lett.* **66**, 1120 (1995).
- <sup>12</sup>B. Laikhtman, *Phys. Rev. B* **44**, 11 260 (1991).
- <sup>13</sup>A.N. Korotkov, D.V. Averin, and K.K. Likarev, *Appl. Phys. Lett.* **62**, 3282 (1993).
- <sup>14</sup>F. Prengel, A. Wacker, and E. Schöll, *Phys. Rev. B* **50**, 1705 (1994).
- <sup>15</sup>L.L. Bonilla, J. Galán, J.A. Cuesta, F.C. Martínez, and J.M. Molera, *Phys. Rev. B* **50**, 8644 (1994).
- <sup>16</sup>H. Schneider, K.v. Klitzing, and K. Ploog, *Superlatt. Microstruct.* **5**, 383 (1989).
- <sup>17</sup>S.H. Kwok, T.B. Norris, L.L. Bonilla, J. Galán, J.A. Cuesta, F.C. Martínez, J.M. Molera, H.T. Grahn, K. Ploog, and R. Merlin, *Phys. Rev. B* **51**, 10 171 (1995).
- <sup>18</sup>F. Capasso, K. Mohammed, and A.Y. Cho, *Appl. Phys. Lett.* **48**, 478 (1986).
- <sup>19</sup>S. Tarucha and K. Ploog, *Phys. Rev. B* **38**, 4198 (1988).
- <sup>20</sup>W. Müller, D. Bertram, H.T. Grahn, K.v. Klitzing, and K. Ploog, *Phys. Rev. B* **50**, 10 998 (1994).
- <sup>21</sup>S.H. Kwok, R. Merlin, H.T. Grahn, and K. Ploog, *Phys. Rev. B* **50**, 2007 (1994).
- <sup>22</sup>G. Bastard, E.E. Mendez, L.L. Chang and L. Esaki, *Phys. Rev. B* **28**, 3241 (1983).
- <sup>23</sup>D.A.B. Miller, D.S. Chemla, T.C. Damen, A.C. Gossard, W. Wiegmann, T.H. Wood, and C.A. Burrus, *Phys. Rev. Lett.* **53**, 2173 (1984).